Proc. Natl. Acad. Sci. USA
Vol. 92, pp. 4224–4228, May 1995
Biochemistry

The structure of *Ascaris* hemoglobin domain I at 2.2 Å resolution: Molecular features of oxygen avidity

(x-ray crystallography/oxygen binding/protoporphyrin IX)

JIAN YANG*, ANDREW P. KLOEK†, DANIEL E. GOLDBERG†‡, AND F. SCOTT MATHEWS*‡

*Department of Biochemistry and Molecular Biophysics, Washington University School of Medicine, St. Louis, MO 63110; and †Howard Hughes Medical Institute, Departments of Molecular Microbiology and Medicine, Washington University School of Medicine and the Jewish Hospital, St. Louis, MO 63110

Communicated by M. F. Perutz, Medical Research Council, Laboratory of Molecular Biology, Cambridge, United Kingdom, February 3, 1995

ABSTRACT **The perienteric hemoglobin of the parasitic nematode *Ascaris* has an exceptionally high affinity for oxygen. It is an octameric protein containing two similar heme-binding domains per subunit, but recombinant constructs expressing a single, monomeric heme-binding domain (domain 1; D1) retain full oxygen avidity. We have solved the crystal structure of D1 at 2.2 Å resolution. Analysis of the structure reveals a characteristic globin fold and illuminates molecular features involved in oxygen avidity of *Ascaris* perienteric hemoglobin. A strong hydrogen bond between tyrosine at position 10 in the B helix (tyrosine-B10) and the distal oxygen of the ligand, combined with a weak hydrogen bond between glutamine-E7 and the proximal oxygen, grips the ligand in the binding pocket. A third hydrogen bond between these two amino acids appears to stabilize the structure. The B helix of D1 is displaced laterally by 2.5 Å when compared with sperm whale myoglobin. This shifts the tyrosine-B10 hydroxyl far enough from liganded oxygen to form a strong hydrogen bond without steric hindrance. Changes in the F helix compared with myoglobin contribute to a tilted heme that may also be important for oxygen affinity.**

The parasitic nematode *Ascaris suum* contains a hemoglobin in its perienteric fluid of exceptionally high affinity for oxygen, $\approx 10^4$ times greater than for mammalian hemoglobins and 10^2 times higher than for mammalian myoglobins (1–3). The protein is an octamer of subunit molecular mass 43 kDa (4, 5); each subunit consists of two equal size globin domains in tandem (6, 7). In addition, each subunit contains a highly charged C-terminal tail of 23 residues, which in part may be responsible for octamerization of the subunits (6, 7). The functional role of *Ascaris* hemoglobin is not clear, since the rate of oxygen release (half-time of several minutes) is too slow for normal delivery.

The two globin domains of *Ascaris* hemoglobin are highly homologous; they have 62% amino acid sequence identity with no insertions or deletions over a stretch of 149 residues (6, 7). The domains are similar to those of a hemoglobin with equally high oxygen affinity from the closely related nematode *Pseudoterranova decipiens* (8). Domain 1 (D1) of *Ascaris* hemoglobin has been cloned and expressed in *Escherichia coli* and shown to be monomeric in solution (9). The spectral properties and oxygen-binding affinity are similar to those of the native octameric hemoglobin, indicating that the oxygen-binding properties are independent of domain association or oligomerization.

The nature of the high oxygen affinity has been studied kinetically by analysis of the protein sequence and by mutagenesis (1–3, 10–12). The rate of oxygen association, with a second-order rate constant of $1.5 \times 10^6\ M^{-1}\cdot s^{-1}$, is 10-fold lower than that of myoglobin, whereas the oxygen dissociation rate ($0.005\ s^{-1}$) is about 3000-fold less than that for myoglobin ($14\ s^{-1}$), indicating a free energy of oxygen binding that is lower by ≈3 kcal/mol.

When compared to other globins, the degree of sequence identity for each of the two domains ranges from 10% to 20%, although good alignment with the globin family is indicated by several criteria (6). There is conservation of 30 of 33 invariant nonpolar sites, correspondence of the heme-linked proximal His, and alignment of certain Pro and Gly residues. Comparison of the nematode globin sequences with that of myoglobin indicates that the two most distinctive differences in the distal heme pocket are the replacement of His by Gln at position E7 (helix notation) and of Leu by Tyr at position B10. His-E7 is the distal His, which is hydrogen bonded to oxygen in oxymyoglobin; Leu-B10, when replaced by Phe in myoglobin, increases its oxygen affinity 10-fold (13), though when replaced by Tyr, the affinity decreases (10), probably due to steric hindrance in the myoglobin pocket.

Evidence for the importance of the B10 and E7 residues in oxygen affinity arises from mutagenesis studies of D1 of *Ascaris* hemoglobin (11, 12). Replacement of Tyr-B10 by Phe or Leu increases the oxygen dissociation rate about 200-fold and 600-fold, respectively, whereas substitution of Gln-E7 by Leu or Ala increases the rate 5-fold and 60-fold, respectively. Kloek *et al.* (11) and De Baere *et al.* (12) have proposed that, compared to myoglobin, the increased affinity for oxygen of the *Ascaris* heme pocket results from formation of two hydrogen bonds to the liganded oxygen molecule, one from Tyr-B10 and the other from Gln-E7.

We report here the crystal structure§ of recombinant *Ascaris* hemoglobin D1. The model demonstrates the overall structural similarity to myoglobin and provides insight into the source of its high oxygen affinity.

MATERIALS AND METHODS

Crystal Growth and Data Collection. Preparation, purification, and crystallization of recombinant D1 have been described (9, 11). Crystals of D1 were grown by vapor diffusion against 10% (wt/vol) PEG 8000 in the presence of 200 mM Li_2SO_4 and 100 mM Tris buffer (pH 8.5). An optical spectrum of redissolved crystals showed them to be in the oxy form. Data were recorded to 2.15 Å resolution on a Hamlin multiwire area detector from one crystal of D1, with overall $R_{sym} = 0.076$ ($R_{sym} = 0.201$ in the highest resolution shell), and were 97.9% complete. The crystal is in space group $P3_121$ with cell parameters $a = b = 63.5$ Å, $c = 69.9$ Å, $\alpha = \beta = 90°$, $\gamma = 120°$ and contains one molecule per asymmetric unit. The position

The publication costs of this article were defrayed in part by page charge payment. This article must therefore be hereby marked "*advertisement*" in accordance with 18 U.S.C. §1734 solely to indicate this fact.

Abbreviation: D1, domain 1.

‡To whom reprint requests should be addressed.

§The atomic coordinates and structure factors have been deposited in the Protein Data Bank, Chemistry Department, Brookhaven National Laboratory, Upton, NY 11973 (access no. 1ASH).

of the iron atom in the asymmetric unit of D1 was located from an anomalous difference Patterson function.

Solution of the Structure. A single-site mercury derivative of D1 was obtained by soaking a crystal in 2 mM $Hg(CN)_2$ for 16 hr. X-ray data were collected to 2.5 Å resolution, also on the area detector, with $R_{sym} = 0.076$, and showed a mean change in structure factor of 24% with respect to the native data. The mercury-binding site was located in the difference Patterson function and refined using the computer program HEAVY (14). Single isomorphous replacement phases were combined with anomalous scattering data from the native and derivative crystals to determine the absolute configuration of the mercury sites and to compute an electron density map of the native protein. The map was improved by solvent flattening (15). Initially, a model of sperm whale myoglobin was fitted to the map; the heme group and most of the main chain atoms could be positioned in the electron density. Several of the side chains were then "mutated" to the *Ascaris* sequence on a Silicon Graphics Indigo workstation using the graphics program TURBO-FRODO (16). Model building was extended to the remaining parts of the *Ascaris* model from $2F_o - F_c$ maps after several stages of refinement. The model was refined in X-PLOR (17) using a combination of simulated annealing and conjugate gradient refinement after which solvent molecules were introduced.

Structure Comparisons. The rms deviation between equivalent residues was computed using the program HOMOLOG (M. G. Rossmann, ref. 18). Coordinates for recombinant sperm whale oxymyoglobin (ref. 19; access no. 2MGM) and the B10 L → F mutant of recombinant sperm whale oxymyoglobin (ref. 13; access no. 2SPN) were obtained from the Protein Data Bank (20).

RESULTS

Structure Analysis. Extensive use of the structure of myoglobin was made during interpretation of the electron density map. Helical segments surrounding the heme group were identified on the basis of the myoglobin structure, and the appropriate amino acids were replaced. Extension of the model building to the nonhelical regions joining these segments was more difficult but eventually successful. Interpretation of the map was particularly difficult in some regions where some or all of the density for some side chains was not visible and positioning of them was somewhat arbitrary. Thirteen residues, all on the surface, showed weak or absent side chain density, even though the main chain density was clear. Ten of these were at the ends of helices or in nonhelical segments and generally corresponded to regions of high main chain temperature factor. In addition, the last three residues at the C terminus of D1 were not visible.

The final model shows good stereochemistry (Fig. 1). The final R factor for *Ascaris* D1 ($R = \Sigma|F_o - F_c|/\Sigma|F_o|$, where F_o and F_c are the observed and calculated structure factors, respectively) is 17.9% for intensities $>3\sigma$ with 60 solvent molecules included. The rms deviation from ideal bond distances and angles are 0.016 Å and 3.17°, respectively.

Structure of the Molecule. Like all globins, D1 is highly helical; it consists of eight helices, A–H (Fig. 2). The structural alignment of D1 and sperm whale myoglobin proposed by De Baere *et al.* (6), based on a number of conserved features within the globin family, is essentially correct (Fig. 3), further verifying the underlying assumptions. When the C^α backbone of D1 and recombinant sperm whale myoglobin (19) are compared, the rms deviation of C^α positions is 1.77 Å for 131 equivalent residues, with five insertions or deletions of 1–4 aa each in the *Ascaris* sequence with respect to myoglobin (Fig. 3). These are located in the AB loop (four-residue insertion), in the CD loop (one-residue deletion), at the beginning of the F helix (three-residue insertion), in the FG loop (one-residue insertion), and in the GH loop (two-residue insertion). Helices B and F differ to the greatest extent between the two structures, with rms deviations of 2.1 and 2.3 Å, respectively, between equivalent C^α positions. The rms deviation for the remaining helices is 1.34 Å.

Heme Binding. After C^α alignment of D1 and myoglobin, the two heme groups are found to be tilted by 9° with respect to one another, and the iron atoms are displaced by about 1.0 Å (Fig. 4). The tilt of the heme group in D1 with respect to myoglobin may be caused by differences in the F helix. In myoglobin, the four residues before F1 also form a helix (sometimes called F′; ref. 23). The combined helix F′–F is bent at residue F1 because residue F3 is Pro, causing the helix to arc away from the heme group. In *Ascaris* D1, F3 is Glu, allowing the entire F helix (which corresponds to F′–F of myoglobin) to remain straight. The side chains at positions Arg-F7 and His-F8 of D1 abut the heme and may contribute to the tilt.

The heme group of *Ascaris* D1 is held in a hydrophobic pocket by coordination to the N^ϵ atom of the proximal His-F8. The heme is in van der Waals contact with four hydrophobic side chains, Phe-CD1, Met-EF8, Trp-G5, and Phe-H15, and the carbonyl oxygens of Leu-C4 and Tyr-C7. Phe-CD1 and Phe-H15 are both retained in myoglobin, whereas the other two are conservative hydrophobic replacements. Both propionates extend to the surface of the molecule.

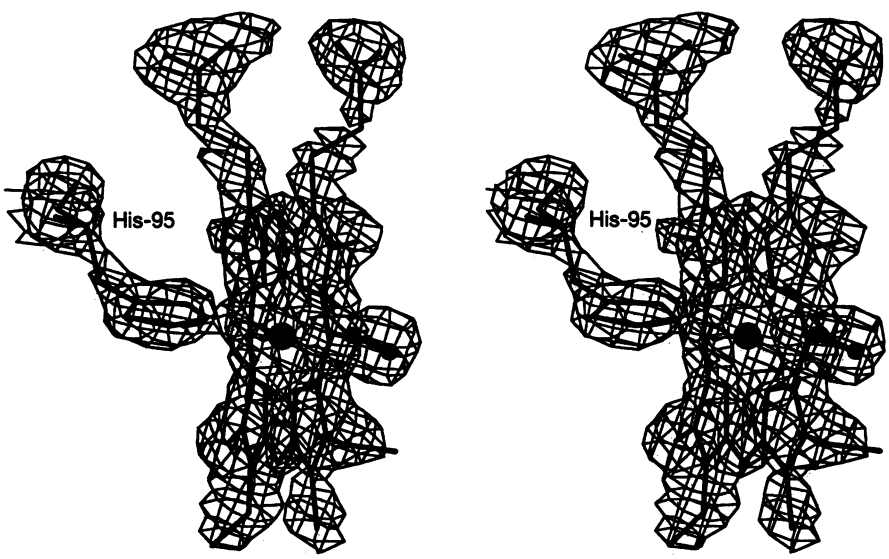

FIG. 1. Stereo diagram of a skeletal model of the heme group, His-95, and dioxygen in *Ascaris* hemoglobin D1 superimposed on the electron density calculated using coefficients $2F_o - F_c$. The electron density map was contoured at 1.5σ.

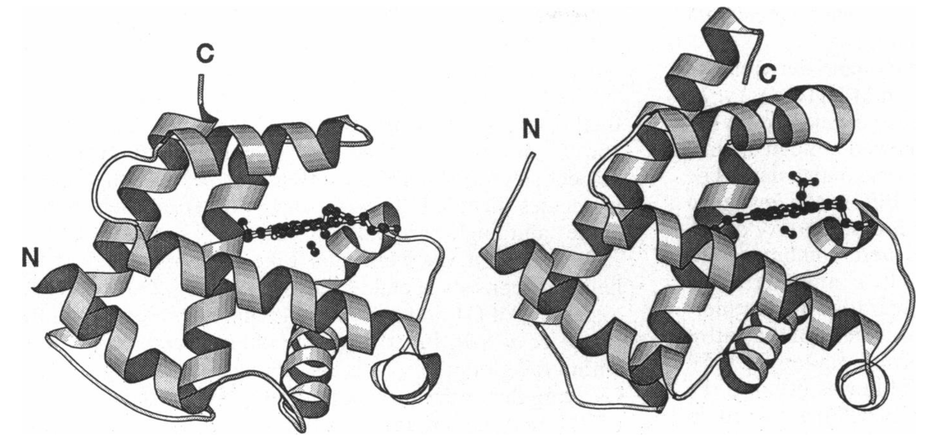

FIG. 2. Molscript diagrams (21) of *Ascaris* hemoglobin D1 (*Left*) and of sperm whale myoglobin (*Right*). The two molecules are in the same relative orientations based on alignment of equivalent C^{α} positions.

The iron atom of D1 lies within 0.03 Å of the heme plane and is coordinated to the four pyrrole nitrogen atoms as well as to O1 of dioxygen at 1.90 Å and to N^{ϵ} of His-F8 at 2.16 Å. These distances are quite similar in oxymyoglobin (19) except that the iron in oxymyoglobin is 0.1 Å further out of the heme plane.

The plane of His-F8 in D1 is rotated by ≈65° about the C^{β}-C^{γ} bond with respect to that of myoglobin (Fig. 4; see also Fig. 5) so that the protons on $C^{\epsilon 1}$ and $C^{\delta 2}$ are nearly staggered with respect to the pyrrole nitrogen atoms of the heme, rather than eclipsed as in the case of myoglobin. Part of the reason for this difference is that N^{δ} of His-F8 in myoglobin forms a bifurcated hydrogen bond to both the carbonyl oxygen of Leu-F4 and to the hydroxyl of Ser-F7, whereas in D1 the His forms only a single hydrogen bond to the carbonyl oxygen atom of Leu-F4 (Fig. 4). In myoglobin, the side chain of Ser-F7 is also hydrogen bonded to the heme propionate group on ring A. In *Ascaris* D1, F7 is Arg, which forms a salt bridge with this heme propionate on the surface of the protein [as predicted by De Baere *et al.* (6)], nearly 8 Å away from His-F8.

Active Site. The oxygen-binding site of D1 in the distal heme pocket is shown schematically in Fig. 6. Since D1 is in the oxy form in the crystal, the ligand of the iron atom was modeled as dioxygen. The dioxygen molecule forms two hydrogen bonds with the protein molecule, in addition to the covalent bond with the ferrous iron atom of the heme group. One hydrogen bond, from the hydroxyl of Tyr-B10 to the distal oxygen (O2), is quite strong, with a hydrogen-bond distance of 2.73 Å. The other hydrogen bond, from Gln-E7 $N^{\epsilon 2}$ to the proximal oxygen (O1), is considerably longer, with a distance of 3.30 Å, and is bifurcated, bonding also to Tyr-B10 O^{η}, at a distance of 2.95 Å. In addition to these two side chains, the dioxygen binding site is surrounded by the hydrophobic side chains of Met-B13, Phe-CD1, and Ile-E11 as well as the heme group.

The active sites of D1 and myoglobin can be compared directly by superimposing the two heme groups. When this is done, the C^{α} backbones of the two structures superimpose less well than previously, with 2.54 Å rms deviation of 132 equivalent positions. The A, B, and D helices differ by 3 Å rms deviation or more between the two structures.

The nearest neighbors to dioxygen (within 6 Å) in D1 and myoglobin are compared in Table 1. The side chains of CD1,

```
                 3 ↓             A-Helix               ↓18
Myoglobin    V L S E G E W Q L V L H V W A K V E A -
Ascaris            N K T R E L C M K S L E H A K V D
                   1 ↑                   ↑     13

                   20↓   B-Helix       B10           35↓36
Myoglobin    - - - D V A G H G Q D I L I R L F K S H
Ascaris      T S N E A R Q D G I D L Y K H M F E N Y
                 ↑20                                 ↑37

             ↓  C-Helix   42↓               51↓ D-Helix
Myoglobin    P E T L E K F D R F K H L K T E A E M K
Ascaris      P P L R K Y F K S R E E Y - T A E D V Q
             ↑38        ↑44                 51↑

             57↓58↓           E7       E-Helix
Myoglobin    A S E D L K K H G V T V L T A L G A I L
Ascaris      N D P F F A K Q G Q K I L L A C H V L C
              ↑58↑  60

             77↓                ↓       86     F-Helix   F8
Myoglobin    K K K G H - - - H E A E L K P L A Q S H
Ascaris      A T Y D D R E T F N A Y T R E L L D R H
              ↑78     81↑

               95↓          100↓         G-Helix
Myoglobin    A T - K H K I P I K Y L E F I S E A I I
Ascaris      A R D H V H M P P E V W T D F W K L F E
               ↑  100       104↑

                     118↓         124↓   H-Helix
Myoglobin    H V L H S R H P G D F G A D A Q G A M N
Ascaris      E Y L G K K T T - L - D E P T K Q A W H
                     ↑   123      126↑

                                               ↓         152
Myoglobin    K A L E L F R K D I A A K Y K E L G Y Q G
Ascaris      E I G R E F A K E I N K (H G R)
                                ↑145
```

FIG. 3. Sequence alignment of *Ascaris* hemoglobin D1 with sperm whale myoglobin based on comparison of their three-dimensional structures. The standard helix definitions for myoglobin are shown above its sequence (solid lines), and the corresponding helices defined by their hydrogen-bonding pattern for *Ascaris* are shown below its sequence. The helix ranges defined by the program DSSP (22) are indicated by vertical arrows for the two sequences. Residues not equivalent when the C^{α} backbones of the two structures were aligned are indicated by italic letters. The key residues B10, E7, and F8 are also indicated.

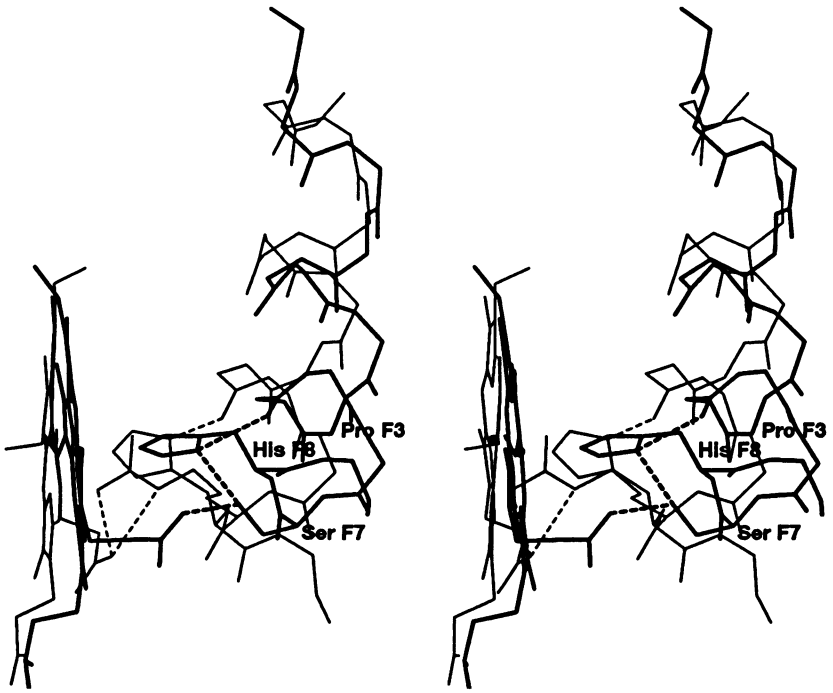

FIG. 4. Stereo diagram (TURBO-FRODO; ref. 16) comparing the F helices and heme groups of *Ascaris* D1 (thin lines) and recombinant sperm whale myoglobin (ref. 19; thick lines). Alignment of the two structures is based on minimization of the rms positional deviations of equivalent C^{α} positions (see text). Helix backbone atoms only are shown except for the side chains of Arg-F7 and His-F8 (*Ascaris*) and of Ser-F7 and His-F8 (myoglobin). Hydrogen bonds and salt bridges from His-F8 N^{δ} to the F5 carbonyl and from Arg-F7 $N^{\epsilon 1}$ and $N^{\eta 2}$ to a heme propionate in *Ascaris* are shown as thin dashed lines. Those from His-F8 N^{δ} to the F5 carbonyl oxygen and to Ser-F7 O^{γ} (bifurcated) and from Ser-F7 O^{γ} to a heme propionate are shown as thick dashed lines. The position of Pro-F3 of myoglobin, which causes helix F′–F to kink, is also indicated.

E7, and E11 (Phe, Gln, and Ile in D1; Phe, His, and Val in myoglobin) are in approximately the same positions in the two structures relative to the heme and oxygen moieties. Met-B13 of D1 substitutes for Ile-G8 of myoglobin as a hydrophobic heme neighbor. Tyr-B10 in D1 is considerably displaced from Leu-B10 of myoglobin, by about 2.5 Å, reflecting the large relative shift in the B helix (Fig. 5). In the B10 L → F mutant of myoglobin (13), the phenyl ring is similarly displaced from Tyr-B10 of D1, again by about 2.5 Å (Fig. 5). A straightforward replacement of Phe by Tyr by computer graphics suggests that in the myoglobin B10 L → Y mutant the Tyr hydroxyl might approach too close to O2 of dioxygen, preventing strong binding of dioxygen.

One other major difference between D1 and myoglobin is the presence of a water molecule, W323, in the myoglobin dioxygen binding pocket, which is located 2.5 Å from O2 and presumably able to form a hydrogen bond to it. No water is found in the interior of D1. However, there is an internal cavity in D1 sufficiently large for a water molecule and centered close to W323 of myoglobin.

DISCUSSION

The enhanced oxygen avidity of *Ascaris* hemoglobin is due to an unusually slow off-rate. This can in large part be explained in terms of the interaction of oxygen with the surrounding protein side chains as found in the D1 crystal structure. There is a strong hydrogen bond from Tyr-B10 O^{η} to O2 of dioxygen and a weak hydrogen bond from Gln-E7 N^{ϵ} to O1 of dioxygen. The latter hydrogen bond is bifurcated with respect to a stronger hydrogen bond from Gln-E7 N^{ϵ} to Tyr-B10 O^{η}. In mutational studies, substitution of Gln-E7 by Leu in *Ascaris* D1 increased the oxygen off-rate 5-fold, compared to a 300- to 600-fold increase when the Tyr-B10 hydroxyl was removed (11, 12). Clearly, the strong hydrogen bond from Tyr-B10 to ligand is the major determinant of oxygen avidity. The distal Gln

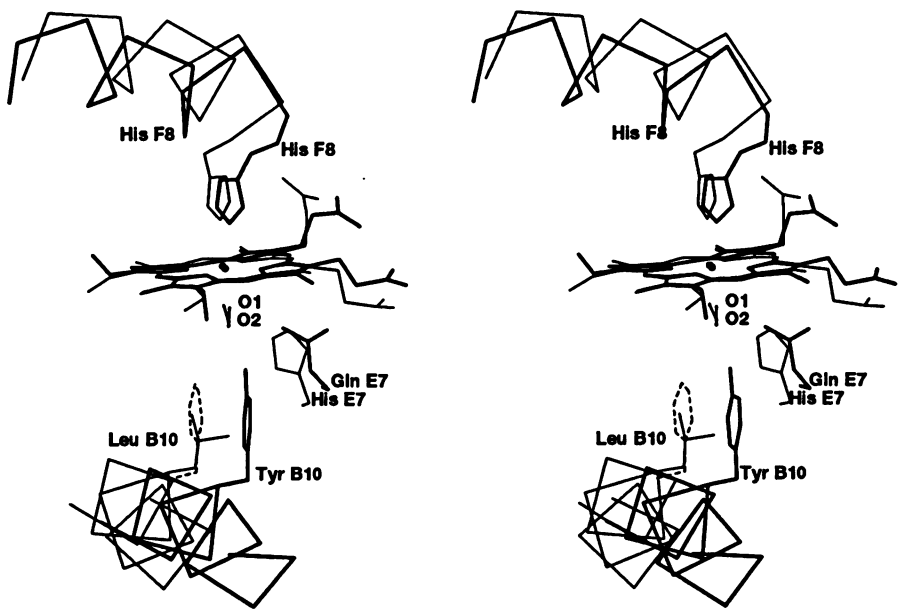

FIG. 5. Stereo diagram of the distal active-site heme pockets of *Ascaris* D1 (thick lines) and recombinant sperm whale myoglobin (thin lines). Alignment of these two structures is based on visual superposition of their heme groups. C^{α} atoms of helices B and F and the side chains of Tyr-B10, Gln-E7, and His-F8 of *Ascaris* and of Leu-B10, His-E7, and His-F8 of myoglobin are shown. The mutant side chain of Phe-B10 (ref. 13; dashed line) is also shown.

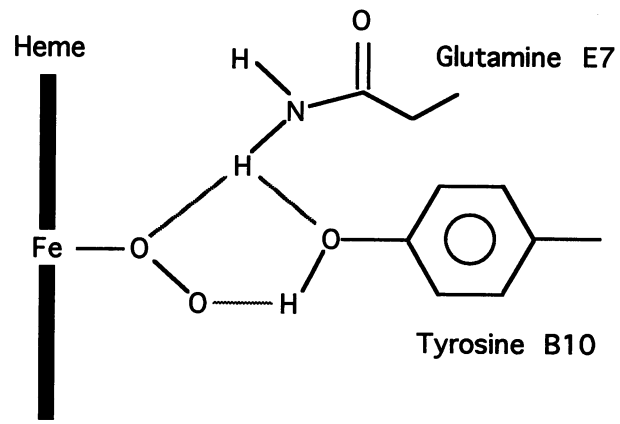

FIG. 6. Schematic diagram of the active-site pocket of *Ascaris* hemoglobin D1. Strong hydrogen bonds from Tyr-B10 to O2 and from Gln-E7 to Tyr-B10 as well as the weak hydrogen bond from Gln-E7 to O1 are shown.

plays a lesser role, and whether the weak hydrogen bond to ligand or the E7 to B10 hydrogen bond is important for the 5-fold enhanced avidity is not clear. In mammalian globins, removing the hydrogen-bonding capacity of the E7 residue (normally His) accelerates the oxygen off-rate from 2-fold (isolated hemoglobin β-chain; ref. 24) to 100-fold (myoglobin; ref. 25). The E7 hydrogen bond to oxygen has been demonstrated directly for sperm whale myoglobin by neutron diffraction (26) in addition to mutagenesis studies (25, 27).

In myoglobin, when Leu-B10 is replaced by Phe, the oxygen dissociation rate drops 10-fold (13). Yet, further substitution by Tyr increases the rate nearly 50-fold (10). This is thought to be due to steric hindrance by the Tyr hydroxyl group. In *Ascaris* D1, the C^{α} position of B10 is displaced by about 2.5 Å from that in myoglobin when the heme groups are superimposed (Fig. 5). This shift is largely parallel to the heme plane, so that the B10 C^{α} to iron distance is only 0.25 Å longer in D1 than in myoglobin, and the B10 C^{α} to dioxygen distance is only 0.1 Å longer. Yet the O^{η} hydrogen of *Ascaris* Tyr-B10 is 0.7 Å further from the dioxygen than that of a myoglobin with Tyr-B10 (modeled on the established Phe-B10 structure of ref. 13). The 2.5 Å lateral shift of the B helix therefore might account for the stabilization of D1 oxygen binding compared to the Tyr-B10 mutant of myoglobin, although strong conclusions cannot be made based on model building.

The *Ascaris* D1 Tyr-B10 would actually be shifted too far away from the ligand, except that the heme is tilted toward the distal pocket, perhaps as a result of F helix substitutions. Compared to myoglobin, His-F8 of *Ascaris* D1 is oriented differently. The more staggered arrangement of the C^{δ} and C^{ϵ} protons of D1 His-F8 with respect to the pyrrole nitrogen atoms could affect the energetics of oxygen binding. The absence of the heme propionate carboxylate from the hydrogen-bonding network of *Ascaris* His-F8 might also influence the oxygen-binding energy by alteration of the local electric field near the heme. Studies of additional *Ascaris* D1 mutants chosen on the basis of the molecular structure reported here will be required to further our understanding of its extraordinary oxygen avidity.

Table 1. Nearest neighbors (<6.0 Å) to dioxygen in the active site of *Ascaris* D1 and myoglobin

Ascaris atom	Ligand atom	Distance, Å	Myoglobin atom	Ligand atom	Distance, Å
Tyr-B10 O^{η}	O2	2.73	Leu-B10 $C^{\delta 2}$	O2	4.87
Met-B13 S^{δ}	O2	5.12	—	—	—
Phe-CD1 C^{ζ}	O2	3.64	Phe-CD1 C^{ζ}	O2	3.22
Gln-E7 $N^{\epsilon 2}$	O1	3.30	His-E7 $N^{\epsilon 2}$	O2	2.72
Ile-E11 C^{δ}	O2	3.77	Val-E11 $C^{\gamma 2}$	O1	3.18
—	—	—	Ile-G8 C^{δ}	O2	5.50
Fe	O1	1.90	Fe	O1	1.93
—	—	—	Solvent 323 O	O2	2.46

We thank Dr. Pedro Alzari for helpful discussion. This research was supported by a grant to D.E.G. from the Lucille P. Markey Charitable Trust and by a grant to F.S.M. from the U.S. Public Health Service (GM20530).

1. Davenport, H. (1949) *Proc. R. Soc. London B* **136,** 271–280.
2. Okazaki, T., Wittenberg, B. A., Briehl, R. W. & Wittenberg, J. B. (1967) *Biochim. Biophys. Acta* **140,** 258–265.
3. Gibson, Q. & Smith, M. (1965) *Proc. R. Soc. London B* **163,** 206–214.
4. Darawshe, S., Tsafadyah, Y. & Daniel, E. (1987) *Biochem. J.* **242,** 689–694.
5. Darawshe, S. & Daniel, E. (1991) *Eur. J. Biochem.* **201,** 169–173.
6. De Baere, I., Liu, L., Moens, L., Van Beeumen, J., Gielens, C., Richelle, J., Trotman, C., Finch, J., Gerstein, M. & Perutz, M. (1992) *Proc. Natl. Acad. Sci. USA* **89,** 4638–4642.
7. Sherman, D. R., Kloek, A. P., Krishnan, R. B. G., Guinn, B. & Goldberg, D. E. (1992) *Proc. Natl. Acad. Sci. USA* **89,** 11696–11700.
8. Dixon, B., Walker, B., Kimmins, W. & Pohajdak, B. (1991) *Proc. Natl. Acad. Sci. USA* **88,** 5655–5659.
9. Kloek, A. P., Yang, J., Mathews, F. S. & Goldberg, D. E. (1993) *J. Biol. Chem.* **268,** 17669–17671.
10. Gibson, Q. H., Regan, R., Olson, J. S., Carver, T. E., Dixon, B., Pohajdak, B., Sharma, P. K. & Vinogradov, S. N. (1993) *J. Biol. Chem.* **268,** 16993–16998.
11. Kloek, A. P., Yang, J., Mathews, F. S., Frieden, C. & Goldberg, D. E. (1994) *J. Biol. Chem.* **269,** 2377–2379.
12. De Baere, I., Perutz, M. F., Kiger, L., Marden, M. C. & Poyart, C. (1994) *Proc. Natl. Acad. Sci. USA* **91,** 1594–1597.
13. Carver, T. E., Brantley, R. E., Jr., Singleton, E. W., Arduini, R. M., Quillin, M. L., Phillips, G. N., Jr., & Olson, J. S. (1992) *J. Biol. Chem.* **267,** 14443–14450.
14. Terwilliger, T. C. & Eisenberg, D. (1983) *Acta Crystallogr. A* **39,** 813–817.
15. Wang, B. C. (1985) *Methods Enzymol.* **115,** 90–112.
16. Roussel, A. & Cambillau, C. (1989) TURBO–FRODO, *Silicon Graphics Geometry Partners Directory* (Silicon Graphics, Mountain View, CA), pp. 77–78.
17. Brünger, A. T. (1992) X-PLOR *Manual* (Yale Univ., New Haven, CT), Version 3.0.
18. Rao, S. T. & Rossmann, M. G. (1973) *J. Mol. Biol.* **76,** 241–256.
19. Phillips, G. N., Arduini, R. M., Springer, B. A. & Sligar, S. G. (1990) *Proteins Struct. Funct. Genet.* **7,** 358–365.
20. Bernstein, F. C., Koetzle, T. F., Williams, G. J. B., Meyer, E. F., Brice, M. D., Rodgers, J. R., Kennard, O., Shimannoucki, T. & Tasumi, M. (1977) *J. Mol. Biol.* **112,** 535–542.
21. Kraulis, P. J. (1991) *J. Appl. Crystallogr.* **24,** 946–950.
22. Kabsch, S. & Sander, C. (1983) *Biopolymers* **22,** 2577–2637.
23. Dickerson, R. E. & Geis, I. (1983) *Hemoglobin: Structure, Function, Evolution, and Pathology* (Benjamin/Cummings, Menlo Park, CA).
24. Mathews, A. J., Rohlfs, R. J., Olson, J. S., Tame, J., Renaud, J.-P. & Nagai, K. N. (1989) *J. Biol. Chem.* **264,** 16573–16583.
25. Springer, B. A. & Sligar, S. G. (1987) *Proc. Natl. Acad. Sci. USA* **84,** 8961–8965.
26. Philips, S. E. V. & Schoenborn, B. P. (1981) *Nature (London)* **292,** 81–92.
27. Olson, S. J., Mathews, A. J., Rohlfs, R. J., Springer, B. A., Egeberg, K. D., Sligar, S. G., Tame, J., Renand, J. P. & Nagai, K. (1988) *Nature (London)* **336,** 265–266.